IEEE Access
Multidisciplinary | Rapid Review | Open Access Journal

Received 6 July 2022, accepted 30 July 2022, date of publication 8 August 2022, date of current version 17 August 2022.

Digital Object Identifier 10.1109/ACCESS.2022.3197587

RESEARCH ARTICLE

Optimizing Symptom Based Testing Strategies for Pandemic Mitigation

TAMÁS PÉNI[1,4], (Member, IEEE), BALÁZS CSUTAK[2], FERENC A. BARTHA[3,4], GERGELY RÖST[3,4], AND GÁBOR SZEDERKÉNYI[2,4], (Member, IEEE)

[1]Institute for Computer Science and Control (SZTAKI), 1111 Budapest, Hungary
[2]Faculty of Information Technology and Bionics, Pázmany Péter Catholic University, 1083 Budapest, Hungary
[3]Bolyai Institute, University of Szeged, 6720 Szeged, Hungary
[4]National Laboratory of Health Security, 6720 Szeged, Hungary

Corresponding author: Tamás Péni (peni@sztaki.hu)

This work was supported in part by the European Union within the framework of the National Laboratory of Health Security under Grant RRF-2.3.1-21-2022-00006, and in part by the National Research, Development and Innovation Fund (NRDI) Fund under Project TKP2021-NVA-09. The work of Balázs Csutak was supported by the Project ÚNKP-21-3-I-PPKE-58. The work of Ferenc A. Bartha was supported in part by the National Research, Development and Innovation Office (NKFIH) under Grant FK 138924; in part by ÚNKP-21-5; and in part by the Bolyai Scholarship of the Hungarian Academy of Sciences. The work of Gábor Szederkényi was supported in part by NKFIH under Grant 131545, and in part by the Hungarian Academy of Sciences under Grant POST-COVID2021-64.

ABSTRACT In this paper, a predictive-control-based approach is proposed for pandemic mitigation with multiple control inputs. Using previous results on the dynamical modeling of symptom-based testing, the testing intensity is introduced as a new manipulable input to the control system model in addition to the stringency of non-pharmaceutical measures. The control objective is the minimization of the severity of interventions, while the main constraints are the bounds on the daily number of hospitalized people and on the total number of available tests. For the control design and simulation, a nonlinear dynamical model containing 14 compartments is used, where the effect of vaccination is also taken into consideration. The computation results clearly show that the optimization-based design of testing intensity significantly reduces the stringency of the measures to be introduced to reach the control goal and fulfill the prescribed constraints.

INDEX TERMS Epidemic modeling, compartmental systems, nonlinear optimization, predictive control.

I. INTRODUCTION

COVID-19 pandemic is one of the biggest challenges the world has been facing with. The virus spreads fast, causes severe disease and easily develops new variants that are more infectious and more resistant to drug treatments than their predecessors. To contain the spread of the virus and reduce the social and economic damage caused by the disease, governments are developing intervention strategies. Choosing a right management policy is a sensitive task where several potentially contradicting objectives have to be taken into consideration. The most important limiting constraint is the capacity of the healthcare system, which can be easily overwhelmed if the spread of the disease is not controlled. It is clear that the transmission of the virus can be efficiently slowed down by appropriate restrictions (social distancing, lockdown), but these measures have negative impacts on the society and the economy that cannot be neglected. These impacts can be reduced by combining the restrictive measures with regular testing (quarantining) and pharmaceutical interventions, e.g. vaccination. The latter also have cost and their availability may be limited. Finding the optimal management policy is therefore a complex problem of balancing between different objectives while several constraints and limitations have to be satisfied.

Reliable quantitative models are of key importance in the development of epidemic management strategy, they are necessary for analyzing, reconstructing and predicting the transmission dynamics of infections. [29], [37], [38]. Naturally, different goals and needs require various modeling approaches with models of different levels of detail and descriptive power [10]. For the tracking of the stochastic process of consecutive infections on an individual level, possibly with detailed spatial information, agent-based models can be

The associate editor coordinating the review of this manuscript and approving it for publication was Ton Duc Do.

used successfully [13], [27], [28]. Another popular direction is the application of artificial intelligence and machine learning for epidemic modeling and prediction [8], [16], [31]. However, the most wide-spread approach is probably the deterministic compartmental framework, where models are given in the form of nonlinear differential equations, usually derived from a susceptible–exposed–infected–recovered (SEIR)-type description [2], [6], [11], [19], [29].

In a control theoretic setup, the epidemic dynamics is considered a system operator which maps inputs to outputs [24]. The inputs contain manipulable components such as the quantified effects of different measures (e.g., social distancing, curfews, lockdowns, quarantine policy) or vaccination, and also non-controllable disturbances like the appearance of a different virus variant or the change of weather. The outputs are typically important observed and/or controlled time-dependent quantities such as the daily and cumulative number of infected or the number of people requiring hospital treatment. Epidemic control design has a huge literature, and majority of the proposed solutions are based on compartmental models given in ODE form [12].

The most frequently targeted control goals are the mitigation or even the complete suppression of the epidemics [14]. The key manipulated input variables for this are the infection rate and the recovery speed if there is any efficient therapy for the disease [22]. Moreover, vaccination intensity can also be considered as a possible input [1], [33]. In addition to the control goals, several important constraints must be taken into consideration related to e.g., the capacity of the healthcare system, the costs of the introduced measures or the tolerance level of the population. A reasonable choice to balance between these often contradicting considerations while still handling the nonlinear dynamics in an appropriate way is the application of model predictive control (MPC) [15], [32]. Social distancing is used as as input in [21] and [20] to suppress the peak of infections together with the minimization of economic loss using the MPC framework. In [24], temporal logic is used for the problem formulation and solution of different scenarios corresponding to the COVID-19 pandemic with complex and possibly time dependent constraints. The computation of an output feedback law was made efficient in [25] by proposing a suboptimal solution requiring convex optimization resulting in a fast solution.

Recent examples from real life show that testing together with an appropriate quarantine policy may have a significant effect in suppressing epidemic waves [18], [30]. China and Taiwan are well-known examples of mass testing, efficient contact tracing and extremely strict quarantining during the COVID-19 pandemic [34]. In Europe, Denmark has successfully applied the combination of intensive testing and other non-pharmaceutical measures to minimize the burden on its healthcare system [41]. However, the effect of testing seems to weaken with the increasing infectiousness of new virus variants such as the Omicron (B.1.1.529). These observations have been mathematically supported and explained by the symptom-based testing model introduced and analyzed in [5].

Based on the above, the aim of this paper is to introduce testing intensity as a manipulable control input in addition to the previously used measures, and explore the corresponding potential benefits and limits in the framework of model predictive control of the COVID-19 pandemic.

II. COMPARTMENTAL MODEL OF TRANSMISSION DYNAMICS

A. MODEL DESCRIPTION

In order to describe the evolution of the COVID-19 epidemic with adequate precision, we create a compartmental model based on the one originally published in [24], with its variations being used in [7] and [26] as well. In the original model, the total population is split into eight compartments: susceptible individuals (x_S), who have not contracted the disease yet, and neither have immunity due to vaccination; latent infected (x_L), who carry the disease, but have no symptoms, and are not yet infectious; asymptomatic (x_A) subjects are infected, but have no symptoms, their infection is not confirmed by testing, and eventually recover without intervention - nevertheless, they can transmit the disease to others; presymptomatic (x_P) people can already infect others, but their symptoms have not appeared yet; symptomatic infected (x_I) present symptoms of the disease, can infect others, and some of them require hospitalization to recover; hospitalised (x_H) patients cannot infect others due to isolation, and might recover or die; recovered (x_R) people are considered to be totally immune to the disease (on the length of the control horizon); and there is a compartment for deceased individuals (x_D). The overall infection rate parameter is written as $(1 - v)\beta$ which includes the effect of disturbances (e.g., varying infectiousness of the virus, seasonal effects, changes in behaviour and mobility of the population) in β, and also that of the introduced measures and restrictions (from mandatory mask wearing to total lockdown) which are considered manipulable within appropriate limits and represented by the scaling term $1 - v$. A more detailed description of the model is available in the original article [24].

In this work, the model developed in [24] is modified to include the effect of vaccinations, and is equipped with a second input (κ), which is the number of symptom-based tests carried out during a unit time interval. Symptom-based test means that people who are developing special, a-priori defined symptoms are selected at high probability for PCR testing. If the test is positive the person is quarantined. Following the concept of [5] the control input enters the model through the transition rate φ defined as follows:

$$\varphi = \kappa \frac{1}{x_I + x_{VI} + \sigma}, \tag{1}$$

where σ is the so called secondary symptom pool, i.e. the proportion of individuals, who are not infected with COVID-19, but produce the same set of symptoms. Comparing (1) with the formula originally introduced in [5], it can be seen that the original formula contains an additional parameter ρ, which

is the probability that an individual from compartment I or VI produces the symptoms on which the testing is based. In our model, we omit this parameter and investigate various choices of the symptom pool using a slightly different methodology as described later in one of the case studies.

People who have been tested positive are quarantined. Therefore, a new compartment x_Q is added for quarantined individuals: these are symptomatic infected people (from x_I), whose infection was confirmed by a test, are legally obliged to stay at a given location, and thus are unable to get in contact with susceptibles and transmit the disease. The rate of transition from x_I to x_Q depends on the intensity of the testing policy (φ).

Also, we have slightly changed the definition of compartment A to adapt the model to the concept of symptom based testing. In our model the 'Asymptomatic' compartment collects those individuals who do not develop the specific set of symptoms on which the testing is based. So in contrast to the original definition used in [24], in the present model, symptomatic individuals may also be admitted to compartment A if their symptoms differ from the a-priori defined symptom set.

Next, a copy is created for compartments x_S, x_L, x_P, x_I, x_Q, with identical meaning, only for those individuals who already have some level of immunity due to vaccination: $x_V, x_{VL}, x_{VP}, x_{VI}, x_{VQ}$ respectively. The possible transitions from these new compartments remain unchanged, only the parameters (e.g., probability of hospitalization) are different. The transition from non-vaccinated compartments to vaccinated ones is determined by parameter γ, standing for the ratio of total population being vaccinated in a unit time interval.

The model may suggest that only the people in compartments S, L, P can get vaccinated. Actually, this is not the case. When a vaccination campaign is carried out, people in A and R compartments can get vaccine as well, since they cannot be distinguished from the members of the other compartments. As the vaccinated Asymptomatic or Recovered individuals remain in their A or R compartments, so they do not influence the transition dynamics. By definition, people in compartment I show symptoms, so they are declared ill, therefore, they are not vaccinated either. The $I \rightarrow VI$ transition can thus be neglected.

The final layout of the model, showing all the compartments, transitions, and the parameters influencing them can be seen in Fig. 1. Formally, the model is described by dynamic equations (2) as follows:

$$\begin{aligned}
\dot{x}_S &= -(1-v)\beta\,(x_P + x_I + x_{VP} + x_{VI} + \ldots \\
&\quad \delta x_A)\,x_S - \gamma x_S && \text{(2a)}\\
\dot{x}_L &= (1-v)\beta\,(x_P + x_I + x_{VP} + x_{VI} + \ldots \\
&\quad \delta x_A)\,x_S - \alpha x_L - \gamma x_L, && \text{(2b)}\\
\dot{x}_P &= \alpha q x_L - \rho_P x_P - \gamma x_P, && \text{(2c)}\\
\dot{x}_I &= \rho_P x_P - \rho_I x_I - \varphi x_I, && \text{(2d)}\\
\dot{x}_Q &= \varphi x_I - \rho_Q x_Q, && \text{(2e)}\\
\dot{x}_V &= -(1-v)(1-V_{\text{eff}})\beta\,(x_P + x_I + \ldots \\
&\quad x_{VP} + x_{VI} + \delta x_A)\,x_V + \gamma x_S, && \text{(2f)}\\
\dot{x}_{VL} &= (1-v)(1-V_{\text{eff}})\beta\,(x_P + x_I + \ldots \\
&\quad x_{VP} + x_{VI} + \delta x_A)\,x_V - \alpha x_{VL} + \gamma x_L && \text{(2g)}\\
\dot{x}_{VP} &= \alpha q_V x_{VL} - \rho_P x_{VP} + \gamma x_P, && \text{(2h)}\\
\dot{x}_{VI} &= \rho_P x_{VP} - \rho_{VI} x_{VI} - \varphi x_{VI}, && \text{(2i)}\\
\dot{x}_{VQ} &= \varphi x_{VI} - \rho_{VQ} x_{VQ}, && \text{(2j)}\\
\dot{x}_A &= \alpha(1-q)x_L + \alpha(1-q_V)x_{VL} - \rho_A x_A, && \text{(2k)}\\
\dot{x}_H &= \rho_I \eta_I x_I + \rho_Q \eta_Q x_Q + \rho_{VI}\eta_V x_{VI} + \ldots \\
&\quad \rho_{VQ}\eta_V x_{VQ} - h x_H, && \text{(2l)}\\
\dot{x}_R &= \rho_A x_A + \rho_I(1-\eta)x_I + \rho_Q(1-\eta)x_Q + \ldots \\
&\quad + \rho_{VI}(1-\eta_V)x_{VI} + \ldots \\
&\quad \rho_{VQ}(1-\eta_{VQ})x_{VQ} + h(1-\mu)x_H, && \text{(2m)}\\
\dot{x}_D &= h\mu x_H, && \text{(2n)}
\end{aligned}$$

It is visible from the above equations that separate birth/death processes are neglected, and the state variables denote the proportion of individuals in the corresponding compartments, i.e. the sum of the state variables is 1 in each time instant. In a more compact form, we can write the system as $\dot{x} = f(x, u)$, with $x = [x_S\ x_L\ x_P\ x_I\ x_Q\ x_V\ x_{VL}\ x_{VP}\ x_{VI}\ x_{VQ}\ x_A\ x_H\ x_R\ x_D]^T$, $u = [v\ \kappa]^T$, and f is standing for the right hand side of the equations. As commonly done in literature, we suppress the time argument t of the variables x and u.

B. MODEL PARAMETERS

Model parameters characterising the transitions among non-vaccinated compartments were set in accordance with related literature [9], [17] with slight modifications to include the effect of measures specific to Hungary [7], [29]. The parameters of the vaccinated compartments are distinguished from the parameters of the non-vaccinated by the V subscript.

The parameters of the "vaccinated" part of model have been chosen based on the following considerations. First, due to the vaccination, the transmission rate of infection (transition $V \rightarrow VL$) is significantly smaller than in the non-vaccinated case. Specifically, we use $\beta(1 - V_{\text{eff}})$ for vaccinated compartments, where V_{eff} is the vaccine efficiency taking values from the interval [0.4, 0.9]. Secondly, since a vaccinated individual is less likely to develop symptoms than a non-vaccinated person, therefore q_V is smaller than q. The nominal value has been chosen by using the related literature (see, e.g. [35], [36]). Thirdly, the probability of hospitalization is also different for the vaccinated and non-vaccinated cases [4], [23]. These specific values have been fine tuned by studying the epidemiological data registered in Hungary. By analysing Hungarian statistical data, we have found that the other parameters of the two model parts can be chosen identical.

There are two new parameters in the model that were not introduced in the earlier model derived in [24]. The first is σ, i.e. the size of the secondary symptom pool. This parameter influences the effectiveness of testing through equation (1).

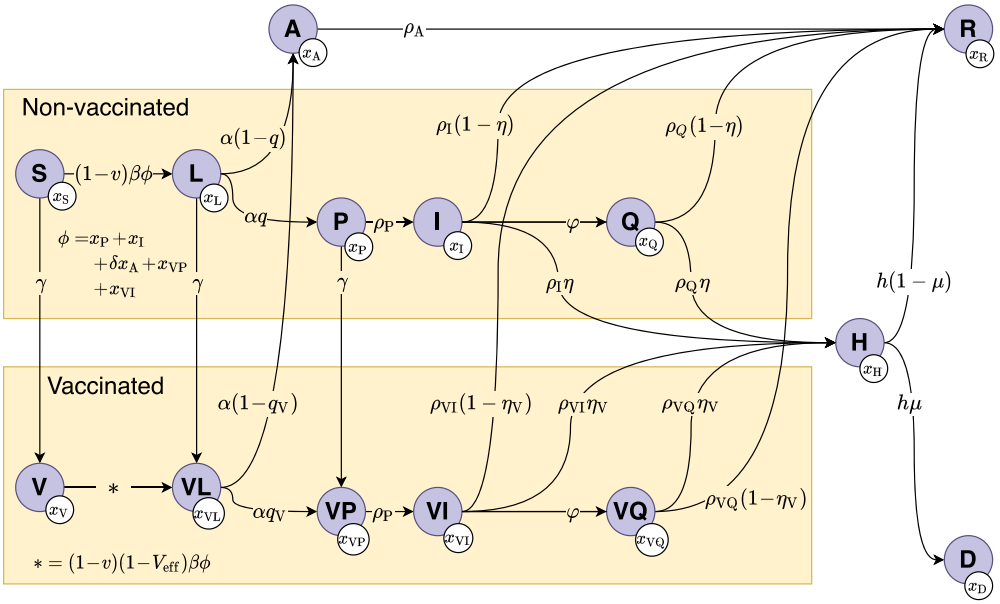

FIGURE 1. Compartmental model.

Predominantly, we assume that testing is based on the whole set of common symptoms of COVID-19. Taking a typical influenza epidemic as a baseline, we set $\sigma = 10^{-3}$ (equivalent to about 10000 individuals) in accordance with the average number of individuals developing similar symptoms without COVID-19 infection. By restricting the symptom set and considering more severe disease progression as a candidate for testing, this value gets smaller. A preliminary analysis of the impact of different σ values on the efficiency of testing is presented in [5].

The next important parameter is γ, that is the rate of vaccination. By analysing the Hungarian statistical data we have chosen for γ to represent a reduced intensity vaccination after the initial vaccination peak, between the lowest and highest values documented. The current value of γ, which is 0.0025, corresponds approximately to 2500 new vaccinated individuals per day.

C. DISCRETIZATION

The control design procedure presented in the next section requires a discrete time model. Therefore the above equations were discretized using the fourth order Runge-Kutta method with sampling time $T_s = 1$ day. Numerical simulations have been carried out with various input signals (v, κ) to verify that the discrete time model approximates the continuous dynamics with sufficient accuracy. The discrete time model is denoted by $F(\cdot)$, that is the dynamical equations can be written in compact form as follows: $x(k+1) = F(x(k), v(k), \kappa(k))$.

III. CONTROL POLICY DESIGN BY NONLINEAR OPTIMIZATION

The aim of a mitigation strategy is to control the epidemic course such that the epidemic peak is reduced and the harmful effects of the disease caused by the virus are minimized. This can be achieved by keeping the population size in certain compartments under a predefined limit. For example, to avoid the overwhelming of healthcare capacity, compartment H is constrained from above by the number of maximum available hospital beds. Since the interventions (social distancing, testing, vaccination, etc.) have social and financial costs, the mitigation goals have to be achieved by using the minimal necessary control actions. To meet all of these requirements a constrained optimization problem can be formulated

TABLE 1. Parameters and values for non-vaccinated (NV) and vaccinated (V) subjects, applied in the simulations.

Parameter NV	Parameter V	Interpretation	Value NV	Value V
β		Transmission rate	0.75	
V_{eff}		Efficiency of vaccination	$0.4 - 0.9$	
α^{-1}		Latent period (days)	2.5	
ρ_{P}^{-1}		Pre-symptomatic infectious period (days)	3	
δ		Relative transmissibility of asymptomatic	0.8	
ρ_{A}^{-1}		Infectious period of asymptomatic (days)	4	
q	q_V	Prob. of developing symptoms	0.6	0.012
ρ_{I}^{-1}	ρ_{VI}^{-1}	Infectious period of symptomatic cases (days)	4	4
ρ_{Q}^{-1}	ρ_{VQ}^{-1}	Quarantine period (days)	4	4
η	η_V	Hospitalization probability of symptomatic cases	0.076	0.0152
h^{-1}		Average length of hospitalization (days)	10	
μ		Probability of fatal outcome, given hospitalization	0.145	
σ		Secondary symptom pool	0.001	
γ		Rate of vaccination	0.0025	
Π		Population size (Hungary)	9 800 000	

as follows:

$$\min_{\mathbf{v},\boldsymbol{\kappa}} \ \frac{1}{\bar{v}^2}\sum_{k=1}^{N} v(k)^2 \tag{3a}$$

w.r.t.

$$x(i+1) = F(x(i), v(j(i)), \kappa(i)),\ x(0) = x_0 \tag{3b}$$

$$i = 0 \dots N+K-1 \tag{3c}$$

$$j(i) = \begin{cases} \lfloor i/L \rfloor & \text{if } i \le N \\ \lfloor N/L \rfloor & \text{if } i > N \end{cases} \tag{3d}$$

$$\kappa(i) = 0, \quad \text{if } i > N \tag{3e}$$

$$0 \le \kappa(i) \le (x_{\mathrm{I}}(i) + x_{\mathrm{VI}}(i) + \sigma) \tag{3f}$$

$$0 \le v(j(i)) \le \bar{v} \tag{3g}$$

$$\sum_{k=0}^{N-1} \kappa(k) \le \bar{\kappa} \tag{3h}$$

$$x_{\mathrm{H}} \le \bar{x}_{\mathrm{H}} \tag{3i}$$

where the notations and variables are explained as follows:

- $\mathbf{v} = [v(0), \dots v(\lfloor N/L \rfloor)]$, $\boldsymbol{\kappa} = [\kappa(0), \dots \kappa(N-1)]$.
- N is the length of the time horizon the input sequence is computed over. Using the concept of model predictive control, the input sequence is determined over a finite time horizon. As k starts from 0, we obtain an input sequence for the time interval $[0, (N-1)\cdot T_s]$. In this paper we take this step and analyse the result obtained. In closed loop control the process could be continued: the first element of the control sequence would be applied to the system for T_s time period, then the state vector x_1 would be measured (or estimated) and the optimization (3) restarts to obtain the next control sequence for time interval $[T_s, N\cdot T_s]$. Feedback control is necessary in real application to attenuate modeling uncertainties and possible measurement noises. In the current study we focus on the analysis and optimization based design of the control policy, therefore we stop after the first step and do not implement a full feedback controller.
- The cost function evaluates the cumulative squared norm of the first control input, which quantifies the non-pharmaceutical measures applied to the society. The aim is to find a control policy that applies only the minimal necessary restrictions. The squared norm of the inputs is normalized by $1/\bar{v}^2$, where $\bar{v}$ is the upper bound of v. $\bar{v}$ corresponds to the strictest measure, which is the total lockdown of the cities (see below). By this normalization, a unit cost is assigned to the total lockdown so the control cost measures the stringency of the interventions relative to the strictest measure. Currently each control action $v(i)$ has the same weight in the cost function, but naturally it is possible to choose different weighting strategy as well.
- K is the length of the safety time window. This is a short (few weeks length) time interval following the control window, where the control input is not updated, but the constraints have to be satisfied. This prevents the optimization to simply improve the cost function by generating less effective (in our case smaller) control actions at the end of the horizon. Turning off the controller in the last few steps leads to high increase in the constrained state variable, which can therefore easily exceed the limit right after leaving the control window. In our case the control action in the safety time window is defined as follows: the first input is kept at its last (N-th) value, the second input (testing) is turned off, i.e. no test is performed after the control horizon.
- Constraint (3g) defines upper and lower bounds for control input v. Setting $v = 0$ corresponds to applying no intervention. The upper bound quantifies the effect of the strictest measure, i.e. the total lockdown of the cities. Based on [40], we have chosen $\bar{v} = 0.8$ for this upper bound.
- Constraint (3f) comes from the definition of κ: the number of tests carried out in a unit time interval cannot be larger than the total number of symptomatic individuals.
- Constraint (3h) describes the assumption that the total number of PCR tests available on the control horizon is a-priori fixed. This maximal value is denoted by $\bar{\kappa}$. The constraint prescribes that the number of all tests performed in the control period should not exceed $\bar{\kappa}$. With this constraint the optimization algorithm tries to find the optimal distribution of available test capacity.
- Parameter L and definition of index j. Since the first control input determines rules and restrictions that have to be performed by the society, it takes time to have impact on the dynamics. Therefore it is of no use changing the control input at each sampling instant. We therefore prescribe that v is updated only at every L-th time step.
- Constraint (3i) introduces an upper bound for the number of hospitalized patients. This is now $\bar{x}_{\mathrm{H}} = 10^{-3}$ corresponding to the maximal number of available hospital beds safely usable for COVID-treatment in Hungary.
- Note that there is no terminal constraints introduced for the final state $x(N)$. In a general MPC design this constraint is used to guarantee recursive feasibility of the optimization and the stability of the closed loop system. In our case this is not necessary for two reasons. First, we focus on the computation of the control policy and do not implement a feedback controller (see the second bullet point above). Second, in the numerical examples we will choose the control horizon N long enough to cover the entire ''lifetime'' of the epidemic: by the end of the control horizon the critical compartments (*SLPA*) will start emptying and the corresponding states converges to zero. The convergence to the origin follows from the structure of the model: the model does not contain feedback branches: the individuals migrate only forward from compartment S to compartments D and H.

The optimization problem to be solved is nonlinear and nonconvex. Finding a solution to it is challenging mainly due to the complexity of the dynamical model and the long

control horizon. To make it easier to solve we take three simplification steps.

- First, state variables x_R and x_D do not affect the dynamics of the others, there are no constraints prescribed for them and they do not appear in the cost. Therefore these two state variables can be removed from the model. The reduced state vector and dynamical model will be denoted by $\tilde{x}$ and $\tilde{F}$, respectively.
- Second, instead of κ, we choose $\varphi = \kappa/(x_I + x_{VI} + \sigma)$ as the input variable. In this way, the rational term $1/(x_I + x_{VI} + \sigma)$ is removed from the optimization problem. To satisfy the constraints prescribed for κ, we first introduce an additional state variable z with the following discrete time dynamics: $z(i+1) = \varphi(i) \cdot (x_I(i) + x_{VI}(i) + \sigma)$. Clearly, z integrates input κ, so $z(N-1) = \sum_{k=0}^{N-1} \kappa(i)$. Therefore, (3h) can be replaced by $z(N-1) \leq \bar{\kappa}$, which is also linear. Although changing the input variable involves a new state with polynomial dynamics, we have found that, this solution is still better from a computational point of view than leaving rational terms in the optimization problem. After determining input sequence φ, the actual control input κ can be obtained by using the formula $\kappa(i) = \varphi(j(i)) \cdot (x_I(i) + x_{VI}(i) + \sigma)$.
- The third modification we make is to replace the hard constraint (3i) with a soft one. For this, a new nonnegative decision variable ε is introduced and added to the right hand side of (3i). This allows for a small violation of the constraint. Large values for ε are penalized in the cost by an additive term $c\varepsilon$, where $c > 0$ is a suitably chosen scaling factor. With the original hard constraint the solver tends to run into infeasibility as x_H approaches its limit. Using the proposed soft constraint this issue can be eliminated.
- Finally, to avoid oscillations in control input κ, we constrained φ to change only weekly, together with v. As x_I and x_{VI} still change daily, this constraint does not imply that κ remains constant for a week, but the control input is suitably smoothed out. The constraint can be interpreted as limiting the percentage of symptomatic patients tested in each week.

The final form of the optimization problem is summarized below.

$$\min_{\mathbf{v},\varphi} \quad \frac{1}{\bar{v}^2} \sum_{i=1}^{N} v(k)^2 + c\varepsilon \tag{4a}$$

w.r.t.

$$\begin{bmatrix} \tilde{x}(i+1) \\ z(i+1) \end{bmatrix} = \begin{bmatrix} \tilde{F}(\tilde{x}(i), v(j(i)), \varphi(j(i))) \\ z(i) + \varphi(j(i))(x_I(i) + x_{VI}(i) + \sigma) \end{bmatrix}, \tag{4b}$$

$$\tilde{x}(0) = \tilde{x}_0 \tag{4c}$$

$$i = 0 \ldots N + K - 1 \tag{4d}$$

$$j(i) = \begin{cases} \lfloor i/L \rfloor & \text{if } i \leq N \\ \lfloor N/L \rfloor & \text{if } i > N \end{cases} \tag{4e}$$

$$\varphi(\lfloor N/L \rfloor) = 0 \tag{4f}$$

$$0 \leq \varphi(j(i)) \leq 1 \tag{4g}$$

$$0 \leq v(j(i)) \leq \bar{v} \tag{4h}$$

$$z(N-1) \leq \bar{\kappa} \tag{4i}$$

$$x_H \leq \bar{x}_H + \varepsilon, \quad \varepsilon \geq 0 \tag{4j}$$

The above problem can be solved in a numerically stable way, for various initial conditions and parameters.

IV. CASE STUDIES

In this section we present control strategies for different epidemic scenarios in order to demonstrate the applicability of the predictive algorithm and draw conclusions about optimal management planning. Three main scenarios are considered: first the effect of vaccination is examined in cases of different vaccine efficiency (subsection IV-A), then the effectiveness of the symptom based testing as a control input is investigated (subsection IV-B). Finally, we analyse the effect of changing the symptom set, on which the testing is based IV-C). In all of the three scenarios the control horizon is $N = 168$ days, the safety period is $K = 30$ days (1 month). We constrain control input v to change only weekly, i.e. $L = 7$. The initial state x_0 for every simulation test is chosen as follows:

$$\begin{aligned} x_L(0) &= 5000/\Pi,\ x_P(0) = 4000/\Pi,\ x_A(0) = 2000/\Pi, \\ x_I(0) &= 100/\Pi,\ x_H(0) = 200/\Pi,\ x_Q(0) = 100/\Pi, \\ x_{VL}(0) &= 200/\Pi,\ x_{VP}(0) = 50/\Pi, \\ x_{VI}(0) &= x_{VQ}(0) = 0, \\ x_R(0) &= x_D(0) = 0, \\ x_V(0) &= \text{depends on the scenario}, \\ x_S(0) &= 1 - \text{“sum of the other states”} \end{aligned}$$

In the cost function the coefficient c penalizing the soft constraint violation is chosen to be $c = 1000$. The optimization problem has been formulated in CasADi [3] and solved by the off-the-shelf nonlinear solver IpOpt [39]. The computations have been performed on a Dell Vostro 5471 laptop equipped with an Intel i7 processor and 8GB RAM. On average, one simulation takes 1-2 minutes to complete. The resulting control input sequence is tested on the continuous time model in open loop configuration by using the ode45 solver of Matlab.

A. TESTING STRATEGIES FOR DIFFERENT STATES OF VACCINATION

In this scenario the optimization problem (4) was solved with different initial values for x_V and V_{eff}. Specifically, $x_V(0) \in \{0.2, 0.3, 0.4, 0.5, 0.6, 0.7, 0.8\}$ and $V_{eff} \in \{0.4, 0.5, 0.6, 0.7, 0.8, 0.9\}$. We examined the impact of the initial vaccination coverage ($x_V(0)$) and vaccine effectiveness on the control strategy and the course of the epidemic. In all cases the optimization returns a feasible solution, i.e. all constraints can be satisfied. The values of the cost function for every studied ($x_V(0)$, V_{eff}) pairs are shown in Fig. 2. It can be seen that initial vaccination is an important factor, as it fundamentally determines the course of the epidemic. On the other hand,

choosing an efficient vaccine is also essential: increasing the efficiency by 0.1 can reduce the total cost to its fifth: see e.g. the row corresponding to $x_V(0) = 5 \cdot 10^6$. The second (bottom) figure of Fig. 2 shows that the total cost depends approximately linearly in both variables.

Figs. 3–6 plot the state evolution and corresponding control inputs in two representative cases: First, the optimization was carried out with a fixed vaccine efficiency of 0.8 and different $x_V(0)$ values (Fig. 3). The significant effect of the ratio of vaccinated people is clear from the plots. With an approximately 60% ratio of vaccinated, we could prescribe a lower constraint for x_H by setting $\bar{H} = 5 \cdot 10^{-4}$. Still, a medium intensity testing is enough to keep the number of hospitalized people well under the predefined limit, and there is no need for further restrictions. Conversely, a low rate of vaccination requires strict measures and intensive testing in parallel to keep the main constraints. Secondly, $x_V(0)$ was fixed and V_{eff} was changed (Fig. 6). As it can be expected, a less efficient vaccine implies the need of significantly stricter measures. Note that in this scenario the upper bound of hospitalized people is reached, and majority of the available tests are used in all cases. Comparing these results with the previous ones suggests that a high vaccination coverage is definitely preferred even with a less efficient vaccine.

In addition, we have run all simulations without precise planning of κ in order to see how important is to systematically design the testing strategy. The results are plotted in Figs. 3–6 by dashed lines. In these scenarios we have designed κ to be approximately constant when maximal testing intensity is reached, and prescribed that the majority of the tests should be used (if possible, i.e. there are sufficient number of infected) by the end of the control horizon. It is visible that the price of not carefully planned testing can be that significantly stricter measures have to be applied on the society. The difference is particularly striking at a medium vaccination coverage, i.e. when $x_V(0) = 0.6$. In this case the total intervention cost can be halved by a carefully planned test strategy. Beside the reduction of the total cost, the high peaks of control input v are avoided as well. This implies that extremely strict interventions (such as the closing of schools or a total lockdown) could be avoided by thoughtful use of testing capacity. It is important to note that the above results were obtained by assuming the least strict quarantine policy when only the officially recorded infected are quarantined.

B. COMPENSATING LESS EFFICIENT VACCINATION BY TESTING

This scenario is focusing on the potential usefulness of symptom based testing. The same set of optimization problems as in the previous section are solved with different upper bounds for the testing capacity. The values of the cost function obtained in the examined 2×36 simulation cases are collected in Fig. 7. We examined whether strict non-pharmaceutical measures (v) induced by the use of a less efficient vaccine can be alleviated by applying more intensive testing. By analysing the results in Fig. 7 it can be seen that testing is an effective

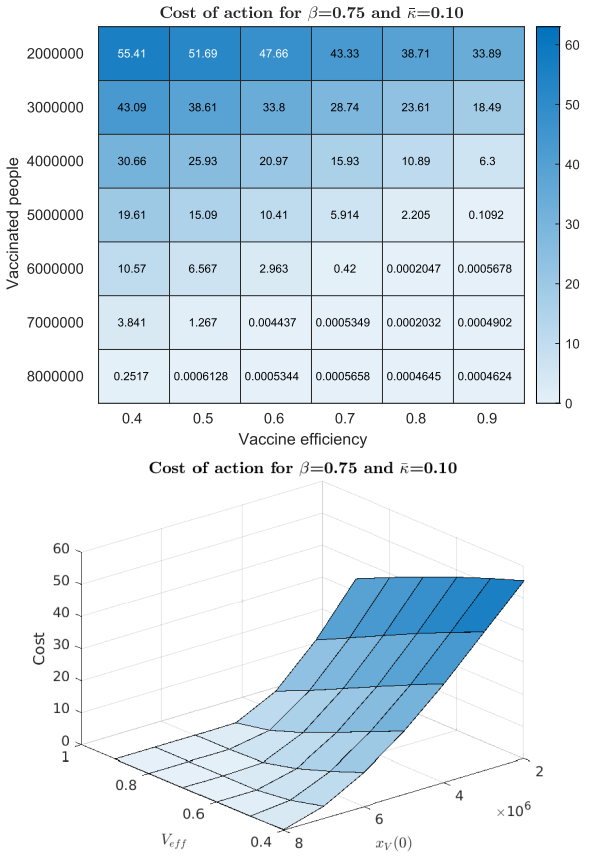

FIGURE 2. Cost of intervention in function of initially vaccinated people and vaccine efficiency (top), with $\beta = 0.75$ (virus variant delta) and $\bar{\kappa} = 0.1$, ie. approximately one million tests available for the length of the control horizon ($N = 168$ days). Three dimensional plot of the cost of intervention (bottom) illustrating the convexity and close to linear nature of the function.

auxiliary control input: if the test capacity is high enough then even a really low (about 20%) vaccination coverage with an average vaccine efficiency can be successfully compensated by intensive testing and quarantining.

Fig. 8 presents the control input and state trajectories in two particular cases selected from the simulations collected in Fig. 7. The first case corresponds to initial values $x_V(0) = 0.4$, $V_{\text{eff}} = 0.5$, $\bar{\kappa} = 0.2$, i.e. a low-efficiency vaccine is applied but large number of test is available. In the second case the initial value of vaccinated compartment is the same ($x_V(0) = 0.4$), but $V_{\text{eff}} = 0.8$ and $\bar{\kappa} = 0.05$, i.e. an efficient vaccine is used but the testing capacity is limited. It can be seen that the values of the cost function in the two cases are very close to each other (0.0558 in the first, and 0.0516 in the second case), i.e. the strictness of the social distancing measures (control input v) is similar. Although a less effective vaccine would result in stricter interventions, this can be avoided by allowing more intensive testing.

C. TESTING STRATEGIES BY MODIFYING THE INDICATOR SYMPTOM

The proposed model is readily capable of studying various testing strategies characterized by the choice of the indicator

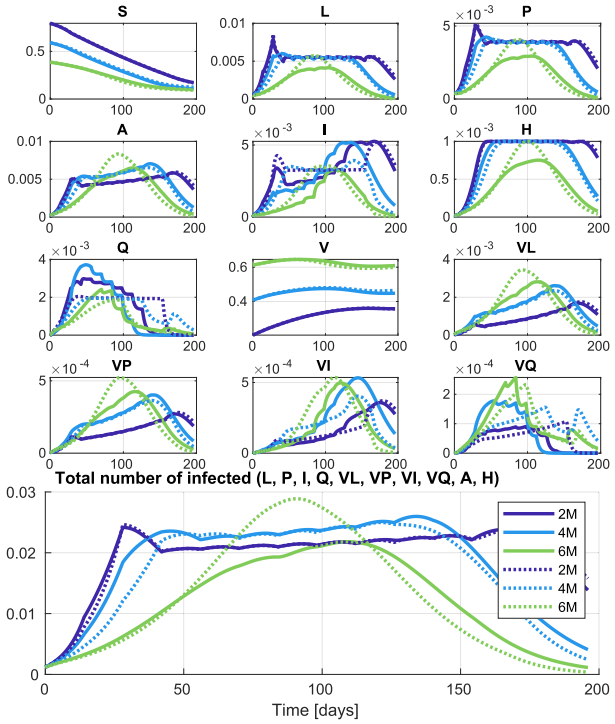

FIGURE 3. Representative figure of the model states and total number of infections, showing the effect of the initial value of the number of vaccinated people, with $\beta = 0.75$, $\bar{\kappa} = 0.1$, and $V_{\text{eff}} = 0.8$. Colors represent values $x_V(0) = 2 \cdot 10^6$ (dark blue), $x_V(0) = 4 \cdot 10^6$ (light blue) and $x_V(0) = 6 \cdot 10^6$ (light green). Dotted lines show the trajectories for the same scenarios, but with approximately constant (non-optimized) κ.

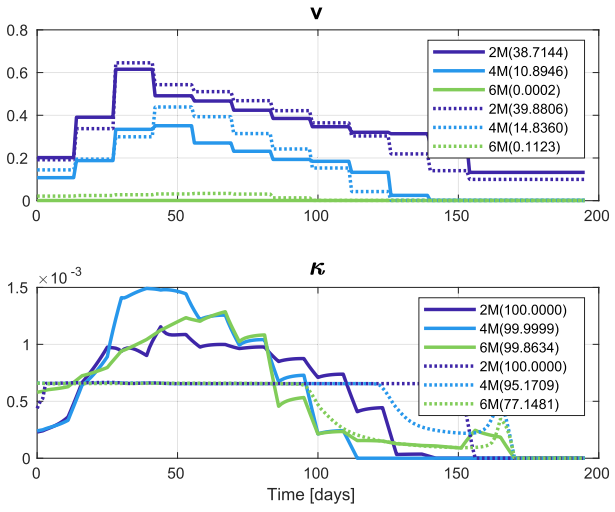

FIGURE 4. Representative figure of the control inputs, showing the effect of the initial value of the number of vaccinated people, with $\beta = 0.75$, $\bar{\kappa} = 0.1$, and $V_{\text{eff}} = 0.8$. Colors represent values $x_V(0) = 2 \cdot 10^6$ (dark blue), $x_V(0) = 4 \cdot 10^6$ (light blue) and $x_V(0) = 6 \cdot 10^6$ (light green). Dotted lines show the optimal inputs for the same scenarios, but with predefined suboptimal testing strategies (additional constraints on κ). We can see the percentage of tests used (compared to the number of tests available) in the legend of the bottom figure. Control costs are shown in parenthesis in the legend of the control input diagram v.

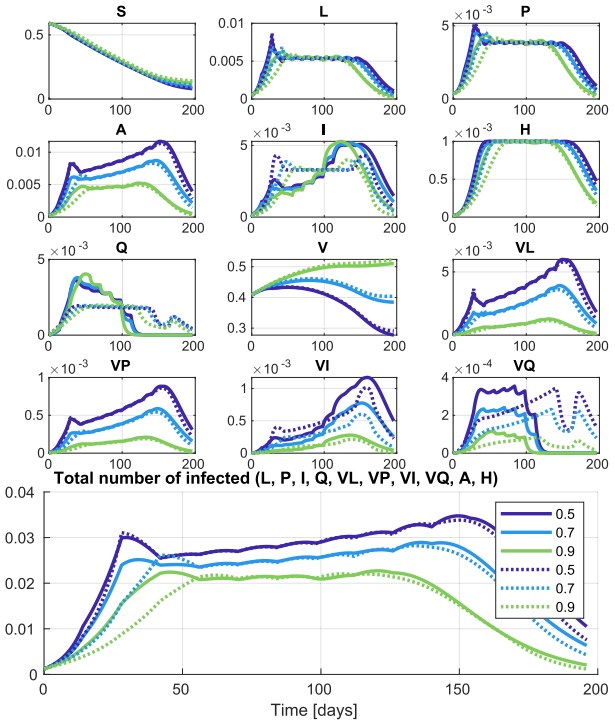

FIGURE 5. Representative figure of the model states and number of infections, showing the effect of vaccine efficiency with $\beta = 0.75$, $\bar{\kappa} = 0.1$, and number of initially vaccinated people $x_V(0) = 4 \cdot 10^6$ (appr. 40% of the population). Colors represent values $V_{\text{eff}} = 0.5$ (dark blue), $V_{\text{eff}} = 0.7$ (light blue) and $V_{\text{eff}} = 0.9$ (light green). Dotted lines show the trajectories for the same scenarios, but with approximately constant (non-optimized) κ.

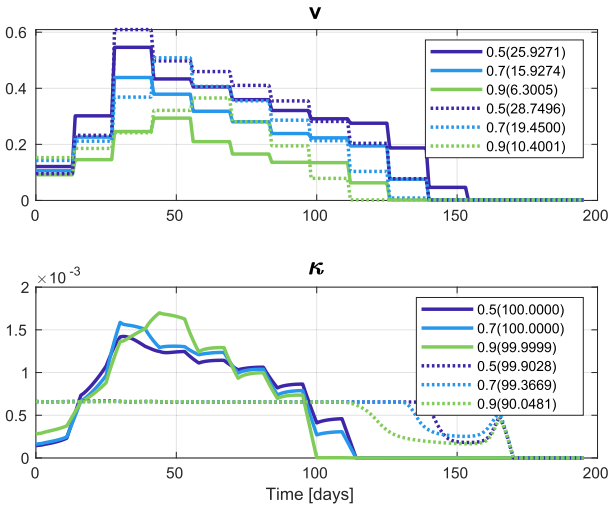

FIGURE 6. Representative figure of the control inputs, showing the effect of vaccine efficiency with $\beta = 0.75$, $\bar{\kappa} = 0.1$, and number of initially vaccinated people $x_V(0) = 4 \cdot 10^6$ (appr. 40% of the population). Colors represent values $V_{\text{eff}} = 0.5$ (dark blue), $V_{\text{eff}} = 0.7$ (light blue) and $V_{\text{eff}} = 0.9$ (light green). Dotted lines show the optimal inputs for the same scenarios, but with predefined suboptimal testing strategies (additional constraints on κ).We can see the percentage of tests used (compared to the number of tests available) in the legend of the bottom figure. Control costs are shown in parenthesis in the legend of the control input diagram v.

symptom as long as the assumption holds that hospitalization is unlikely for other symptomatic infections. A change from the whole set of common symptoms to a more severe disease course will affect the model parametrization in numerous

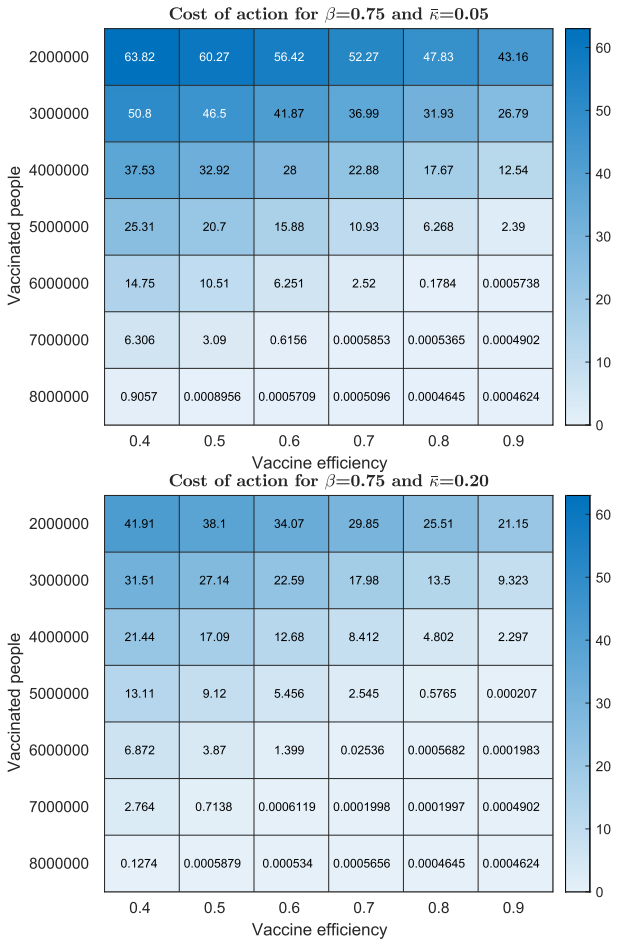

FIGURE 7. Comparison of the values of the cost function, if different number of tests are available: $\bar{\kappa} = 0.05$ (left) and $\bar{\kappa} = 0.2$ (right). Properly divided over the length of the horizon, higher number of tests can significantly reduce the cost, and thus compensate for a less efficient vaccine.

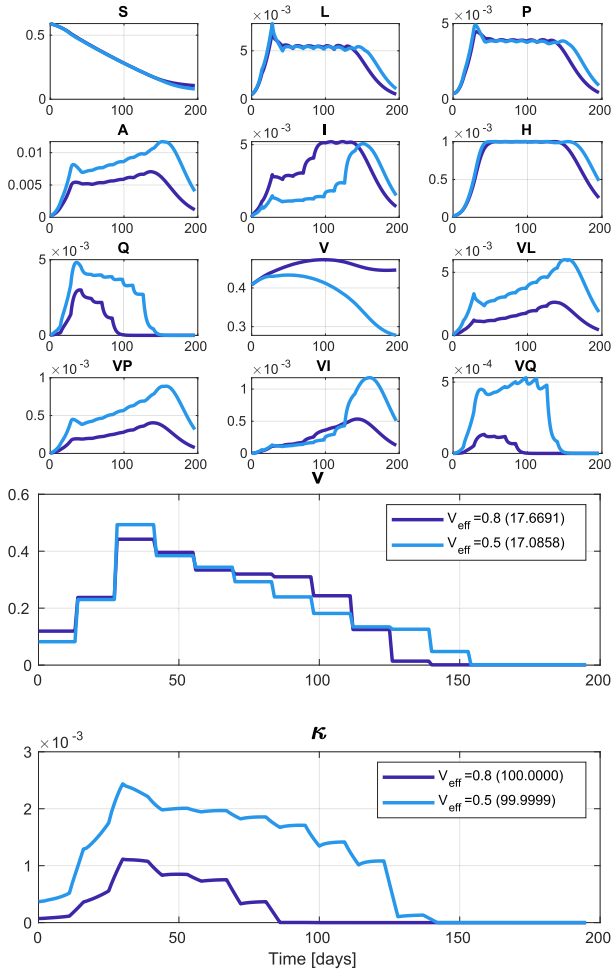

FIGURE 8. Comparison of model states (top) and control inputs (bottom) for two scenarios with similar intervention cost: strong vaccine and low amount of tests ($V_{\text{eff}} = 0.8$, $\bar{\kappa} = 0.05$, dark blue) against weak vaccine and high amount of tests ($V_{\text{eff}} = 0.5$, $\bar{\kappa} = 0.2$, light blue). Control costs are shown in parenthesis in the figure of v, next to the V_{eff} parameter values.

ways. On the positive side, the secondary symptom pool shrinks, hence, the raw testing efficacy is increased. Nevertheless, by channeling more individuals to the A branch will increase its relative transmissibility and average infectious period. Moreover, that branch is not subject to testing, hence, more infections can stay potentially undetected. Finally, the infecteds in the (indicator) symptomatic I branch have an increased possibility of hospitalization corresponding to a more severe disease course.

We investigated a plausible scenario by introducing a new parameter ζ to the model capturing the probability that a symptomatic infected displays the indicator symptom. The baseline corresponding to the parametrization in Table 1 is $\zeta = 1$. As in the model q itself represents the probability of developing indicator symptom and η is the probability of hospitalization thereafter, it is straightforward to see that they are directly and inversely proportional with ζ, respectively. The change in relative infectivity δ may be obtained as a weighted average of the baseline δ and 1 (the latter being the relative infectivity of the I branch wrt. to itself) with weights $(1-q)/(1-q\zeta)$ and $(q-q\zeta)/(1-q\zeta)$ referring to the original A branch and the newly redirected individuals, respectively. The effect on the infectious period of the A branch ρ_{A} may be treated analogously. Summarizing these basic considerations lead to the following adjustment of the aforementioned parameters as functions of ζ.

$$
\begin{aligned}
q(\zeta) &= q \cdot \zeta, \\
\eta(\zeta) &= \eta/\zeta, \\
\delta(\zeta) &= \frac{\delta(1-q) + q(1-\zeta)}{1-q\cdot\zeta}, \\
\rho_{\text{A}}(\zeta) &= \frac{\rho_{\text{A}}(1-q) + \frac{1}{\rho_{\text{P}}^{-1}+\rho_{\text{I}}^{-1}} q(1-\zeta)}{1-q\cdot\zeta},
\end{aligned}
$$

where $q, \eta, \delta, \rho_{\text{A}}, \rho_{\text{P}}, \rho_{\text{I}}$ on the right hand side of the equations refer to the baseline values presented in Table 1. We assumed that a change of $\zeta = 0.75$ results in the shrinking of the secondary symptom pool σ from

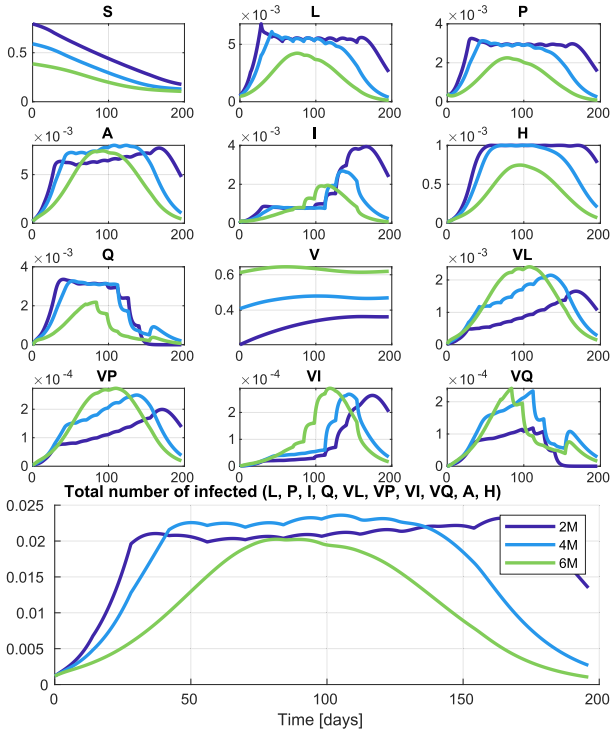

FIGURE 9. Representative figure of the model states and total number of infections, showing the effect of the initial value of the number of vaccinated people using an altered indicator symptom characterized by $\zeta = 0.75$ and $\sigma = 10^{-4}$ with parameters $\beta = 0.75$, $\bar{\kappa} = 0.1$, and $V_{\text{eff}} = 0.8$. Colors represent values $x_V(0) = 2 \cdot 10^6$ (dark blue), $x_V(0) = 4 \cdot 10^6$ (light blue) and $x_V(0) = 6 \cdot 10^6$ (light green).

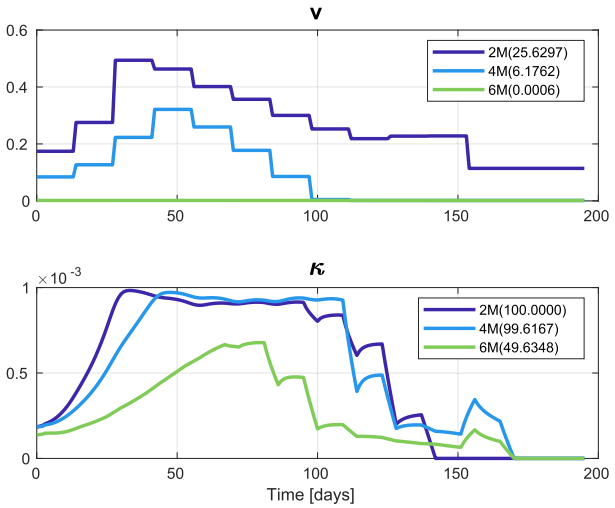

FIGURE 10. Representative figure of the control inputs, showing the effect of the initial value of the number of vaccinated people using an altered indicator symptom characterized by $\zeta = 0.75$ and $\sigma = 10^{-4}$ with parameters $\beta = 0.75$, $\bar{\kappa} = 0.1$, and $V_{\text{eff}} = 0.8$. Colors represent values $x_V(0) = 2 \cdot 10^6$ (dark blue), $x_V(0) = 4 \cdot 10^6$ (light blue) and $x_V(0) = 6 \cdot 10^6$ (light green). We can see the percentage of tests used (compared to the number of tests available) in the legend of the bottom figure. Control costs are shown in parenthesis in the legend of the control input diagram v.

10^{-3} to 10^{-4} and collected the results of the simulations in Figs. 9 and 10. Comparing with Fig. 3, we observe a potential for overall cost reduction due to a more optimal choice of the indicator symptom.

V. CONCLUSION

A control theoretic approach for the management of pandemic mitigation was proposed in this paper. The main idea behind the methodology is the integrated design of non-pharmaceutical measures and testing intensity. Therefore, the testing effort is introduced as an additional manipulable input of the control model, thus a multivariable nonlinear control problem is defined. The dynamical description of symptom-based testing was adopted from [5]. The epidemic model used for the computations is in nonlinear ODE form containing 14 compartments. It includes a simplified model of vaccination as well. The model is parameterized using the literature and Hungarian statistical data on the COVID-19 pandemic. The design goal is the minimization of the unwanted effects of the restrictive measures, while the constraints are focused on the maximum tolerable burden of the healthcare system and the total available number of tests. These somewhat contradicting aspects are handled within the framework of nonlinear model predictive control, which requires the solution of a constrained nonlinear optimization problem. Several scenarios have been studied with different vaccination coverages, different possible vaccine efficiencies and various choices of the indicator symptom. The obtained computation results clearly show that the integrated design can efficiently reduce the severity of non-pharmaceutical measures. It has also been shown that reduced vaccine efficiency or a lower vaccine coverage can be successfully compensated by appropriately scheduled testing. Finally, the effect of changing the indicator symptoms is investigated. It has been shown, that careful selection of the symptom set can further enhance the overall cost reduction. These results clearly prove that testing can be an important auxiliary control input in pandemic management even if the available number of tests is limited.

Although the proposed epidemic model has been constructed with careful considerations, there is a room for refinement. Firstly, in the current model only a simplified vaccination dynamics are used due to the assumption that majority of the vaccinations have already been taken place before the studied epidemic waves. Secondly, the waning of immunity after vaccination or infection is not taken into consideration which is an acceptable approximation for the modeled roughly half year long time interval. Thirdly, quarantining affects only infected individuals in the model which suggests that testing can be an even more efficient control input with stricter quarantine policies. Finally, we do not analyse the effects of parameter uncertainties and measurement noises. By revising the modeling assumptions, the dynamics can be modified and thus enabled to describe more subtle dynamic behavior. After a precise robustness and sensitivity analysis, the control synthesis can be completed with robustness guarantees. These topics will be part of the future research.

REFERENCES

[1] S. Alonso-Quesada, M. De la Sen, R. Agarwal, and A. Ibeas, "An observer-based vaccination control law for an SEIR epidemic model based on feedback linearization techniques for nonlinear systems," *Adv. Difference Equ.*, vol. 2012, no. 1, pp. 1–32, Dec. 2012.

[2] R. M. Anderson and R. M. May, "Population biology of infectious diseases: Part I," *Nature*, vol. 280, no. 5721, pp. 361–367, Aug. 1979.

[3] J. A. E. Andersson, J. Gillis, G. Horn, J. B. Rawlings, and M. Diehl, "CasADi: A software framework for nonlinear optimization and optimal control," *Math. Program. Comput.*, vol. 11, no. 1, pp. 1–36, Jul. 2018.

[4] P. Bager, J. Wohlfahrt, J. Fonager, M. Rasmussen, M. Albertsen, T. Y. Michaelsen, C. H. Møller, S. Ethelberg, R. Legarth, and M. S. F. Button, "Risk of hospitalisation associated with infection with SARS-CoV-2 lineage B.1.1.7 in Denmark: An observational cohort study," *Lancet Infectious Diseases*, vol. 21, no. 11, pp. 1507–1517, 2021.

[5] F. A. Bartha, J. Karsai, T. Tekeli, and G. Röst, "Symptom-based testing in a compartmental model of COVID-19," in *Analysis of Infectious Disease Problems (Covid-19) and Their Global Impact*. Singapore: Springer, 2021, pp. 357–376.

[6] F. Brauer, "Compartmental models in epidemiology," in *Mathematical Epidemiology*. Berlin, Germany: Springer, 2008, pp. 19–79.

[7] B. Csutak, P. Polcz, and G. Szederkenyi, "Computation of COVID-19 epidemiological data in Hungary using dynamic model inversion," in *Proc. IEEE 15th Int. Symp. Appl. Comput. Intell. Informat. (SACI)*, May 2021, pp. 91–96.

[8] S. Ghafouri-Fard, H. Mohammad-Rahimi, P. Motie, M. Minabi, M. Taheri, and S. Nateghinia, "Application of machine learning in the prediction of COVID-19 daily new cases: A scoping review," *Heliyon*, vol. 7, no. 10, Oct. 2021, Art. no. e08143.

[9] G. Giordano, F. Blanchini, R. Bruno, P. Colaneri, A. Di Filippo, A. Di Matteo, and M. Colaneri, "Modelling the COVID-19 epidemic and implementation of population-wide interventions in Italy," *Nature Med.*, vol. 26, no. 6, pp. 855–860, Jun. 2020.

[10] K. Hangos and I. Cameron, *Process Modelling and Model Analysis*. New York, NY, USA: Academic, 2001.

[11] S. He, Y. Peng, and K. Sun, "SEIR modeling of the COVID-19 and its dynamics," *Nonlinear Dyn.*, vol. 101, no. 3, pp. 1667–1680, Aug. 2020.

[12] E. A. Hernandez-Vargas, *Modeling and Control of Infectious Diseases in the Host: With MATLAB and R*. New York, NY, USA: Academic, 2019.

[13] N. Hoertel, M. Blachier, C. Blanco, M. Olfson, M. Massetti, M. S. Rico, F. Limosin, and H. Leleu, "A stochastic agent-based model of the SARS-CoV-2 epidemic in France," *Nature Med.*, vol. 26, no. 9, pp. 1417–1421, Sep. 2020.

[14] C.-H. Hsieh, "On robust economic control of epidemics with application to COVID-19," *IEEE Access*, vol. 9, pp. 167948–167958, 2021.

[15] J. Köhler, L. Schwenkel, A. Koch, J. Berberich, P. Pauli, and F. Allgöwer, "Robust and optimal predictive control of the COVID-19 outbreak," *Annu. Rev. Control*, vol. 51, pp. 525–539, 2021.

[16] S. Lalmuanawma, J. Hussain, and L. Chhakchhuak, "Applications of machine learning and artificial intelligence for COVID-19 (SARS-CoV-2) pandemic: A review," *Chaos, Solitons Fractals*, vol. 139, Oct. 2020, Art. no. 110059.

[17] A. Leontitsis, A. Senok, A. Alsheikh-Ali, Y. Al Nasser, T. Loney, and A. Alshamsi, "SEAHIR: A specialized compartmental model for COVID-19," *Int. J. Environ. Res. Public Health*, vol. 18, no. 5, p. 2667, Mar. 2021.

[18] L. C. Lopes-Júnior, E. Bomfim, D. S. C. D. Silveira, R. M. Pessanha, S. I. P. C. Schuab, and R. A. G. Lima, "Effectiveness of mass testing for control of COVID-19: A systematic review protocol," *BMJ Open*, vol. 10, no. 8, Aug. 2020, Art. no. e040413.

[19] R. M. May and R. M. Anderson, "Population biology of infectious diseases: Part II," *Nature*, vol. 280, no. 5722, pp. 455–461, Aug. 1979.

[20] M. M. Morato, S. B. Bastos, D. O. Cajueiro, and J. E. Normey-Rico, "An optimal predictive control strategy for COVID-19 (SARS-CoV-2) social distancing policies in Brazil," *Annu. Rev. Control*, vol. 50, pp. 417–431, 2020.

[21] M. M. Morato, I. M. L. Pataro, M. V. Americano da Costa, and J. E. Normey-Rico, "A parametrized nonlinear predictive control strategy for relaxing COVID-19 social distancing measures in Brazil," *ISA Trans.*, vol. 124, pp. 197–214, May 2022.

[22] C. Nowzari, V. M. Preciado, and G. J. Pappas, "Analysis and control of epidemics: A survey of spreading processes on complex networks," *IEEE Control Syst.*, vol. 36, no. 1, pp. 26–46, Feb. 2016.

[23] T. Nyberg *et al.*, "Comparative analysis of the risks of hospitalisation and death associated with SARS-CoV-2 omicron (B.1.1.529) and delta (B.1.617.2) variants in England: A cohort study," *Lancet*, vol. 399, no. 10332, pp. 1303–1312, 2022.

[24] T. Péni, B. Csutak, G. Szederkényi, and G. Röst, "Nonlinear model predictive control with logic constraints for COVID-19 management," *Nonlinear Dyn.*, vol. 102, no. 4, pp. 1965–1986, Dec. 2020.

[25] T. Péni and G. Szederkényi, "Convex output feedback model predictive control for mitigation of COVID-19 pandemic," *Annu. Rev. Control*, vol. 52, pp. 543–553, 2021.

[26] P. Polcz, B. Csutak, and G. Szederkényi, "Reconstruction of epidemiological data in Hungary using stochastic model predictive control," *Appl. Sci.*, vol. 12, no. 3, p. 1113, Jan. 2022.

[27] I. Z. Reguly, D. Csercsik, J. Juhász, K. Tornai, Z. Bujtár, G. Horváth, B. Keömley-Horváth, T. Kós, G. Cserey, K. Iván, S. Pongor, G. Szederkényi, G. Röst, and A. Csikász-Nagy, "Microsimulation based quantitative analysis of COVID-19 management strategies," *PLOS Comput. Biol.*, vol. 18, no. 1, Jan. 2022, Art. no. e1009693.

[28] R. J. Rockett *et al.*, "Revealing COVID-19 transmission in Australia by SARS-CoV-2 genome sequencing and agent-based modeling," *Nature Med.*, vol. 26, no. 9, pp. 1398–1404, Sep. 2020.

[29] G. Röst, F. A. Bartha, N. Bogya, P. Boldog, A. Dénes, T. Ferenci, K. J. Horváth, A. Juhász, C. Nagy, T. Tekeli, Z. Vizi, and B. Oroszi, "Early phase of the COVID-19 outbreak in Hungary and post-lockdown scenarios," *Viruses*, vol. 12, no. 7, p. 708, Jun. 2020.

[30] M. Salath, L. Ch Althaus, R. Neher, S. Stringhini, E. Hodcroft, J. Fellay, M. Zwahlen, G. Senti, M. Battegay, A. Wilder-Smith, I. Eckerle, M. Egger, and N. Low, "COVID-19 epidemic in Switzerland: On the importance of testing, contact tracing and isolation," *Swiss Med. Weekly*, vol. 150, pp. 1–3, 2020.

[31] M. S. Satu, K. C. Howlader, M. Mahmud, M. S. Kaiser, S. M. Shariful Islam, J. M. W. Quinn, S. A. Alyami, and M. A. Moni, "Short-term prediction of COVID-19 cases using machine learning models," *Appl. Sci.*, vol. 11, no. 9, p. 4266, May 2021.

[32] F. Sélley, Á. Besenyei, I. Z. Kiss, and P. L. Simon, "Dynamic control of modern, network-based epidemic models," *SIAM J. Appl. Dyn. Syst.*, vol. 14, no. 1, pp. 168–187, Jan. 2015.

[33] O. Sharomi and T. Malik, "Optimal control in epidemiology," *Ann. Operations Res.*, vol. 251, no. 1, pp. 55–71, 2017.

[34] R. Steinbrook, "Contact tracing, testing, and control of COVID-19 – learning from Taiwan," *JAMA Internal Med.*, vol. 180, no. 9, pp. 1163–1164, 2020.

[35] L. Tang, D. R. Hijano, A. H. Gaur, T. L. Geiger, E. J. Neufeld, J. M. Hoffman, and R. T. Hayden, "Asymptomatic and symptomatic SARS-CoV-2 infections after BNT162b2 vaccination in a routinely screened workforce," *Jama*, vol. 325, no. 24, pp. 2500–2502, 2021.

[36] M. G. Thompson, E. Stenehjem, and S. Grannis, "Effectiveness of COVID-19 vaccines in ambulatory and inpatient care settings," *New England J. Med.*, vol. 385, no. 15, pp. 1355–1371, 2021.

[37] O. Tutsoy, S. Colak, A. Polat, and K. Balikci, "A novel parametric model for the prediction and analysis of the COVID-19 casualties," *IEEE Access*, vol. 8, pp. 193898–193906, 2020.

[38] A. Vespignani, H. Tian, C. Dye, J. O. Lloyd-Smith, R. M. Eggo, M. Shrestha, S. V. Scarpino, B. Gutierrez, M. U. G. Kraemer, J. Wu, K. Leung, and G. M. Leung, "Modelling COVID-19," *Nature Rev. Phys.*, vol. 2, no. 6, pp. 279–281, 2020.

[39] A. Wächter and L. T. Biegler, "On the implementation of an interior-point filter line-search algorithm for large-scale nonlinear programming," *Math. Program.*, vol. 106, no. 1, pp. 25–57, Apr. 2005.

[40] H. Wang, Z. Wang, Y. Dong, R. Chang, C. Xu, X. Yu, S. Zhang, L. Tsamlag, M. Shang, J. Huang, Y. Wang, G. Xu, T. Shen, X. Zhang, and Y. Cai, "Phase-adjusted estimation of the number of coronavirus disease 2019 cases in wuhan, China," *Cell Discovery*, vol. 6, no. 1, pp. 1–8, Dec. 2020.

[41] E. A. Yarmol-Matusiak, L. E. Cipriano, and S. Stranges, "A comparison of COVID-19 epidemiological indicators in sweden, norway, denmark, and Finland," *Scandin. J. Public Health*, vol. 49, no. 1, pp. 69–78, Feb. 2021.

TAMÁS PÉNI (Member, IEEE) received the M.Sc. degree in informatics and the Ph.D. degree in electrical engineering from the Budapest University of Technology and Economics, Hungary, in 1999 and 2009, respectively. He is currently a Senior Research Fellow at the Institute for Computer Science and Control (SZTAKI), Eötvös Lóránd Research Network (ELKH), Hungary. His main research interests include predictive control design for nonlinear and linear parameter varying systems, numerical optimization, and machine learning.

BALÁZS CSUTAK received the B.Sc. and M.Sc. degrees in computer science and engineering from Pázmány Péter Catholic University, Budapest, Hungary, where he is currently pursuing the Ph.D. degree in computer science. From 2018 to 2021, he has worked as a Developer of ELKH-SZTAKI, Institute for Computer Science and Control. His research interests include analysis and control of nonlinear dynamic systems, with emphasis on compartmental models, temporal logic and optimization-based estimation and control, and their application on epidemic models.

FERENC A. BARTHA received the M.Sc. degree in mathematics from the University of Szeged, Hungary, in 2008, and the Ph.D. degree from the University of Bergen, Norway, in 2013. Then, he has worked as a Research Scientist at Rice University, Houston, TX, USA. Since 2017, he has been working as an Assistant Professor at the University of Szeged. His research interests include delay systems, resource-aware systems, validated numerical methods, and epidemics modeling.

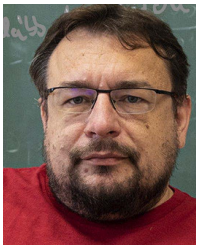

GERGELY RÖST received the Ph.D. degree (Hons.) in mathematics from the University of Szeged, Hungary, in 2006, Promotio Sub Auspiciis. He is currently an Associate Professor with the University of Szeged. Earlier, he was a MITACS Postdoctoral Research Fellow at York University, Toronto; a Research Fellow of the Hungarian Academy of Sciences; a Fulbright Scholar at Arizona State University, Tempe; and a MSCA Research Fellow at the University of Oxford. He is also the Chair of applied and numerical mathematics and the Vice-Head of the Bolyai Institute, University of Szeged. His research interests include the functional differential equations and nonlinear dynamics and their applications in biological systems and mostly infectious disease modeling. He founded the first mathematical epidemiology research group in the country, which was a main basis of the COVID-19 modeling efforts in Hungary throughout the pandemic.

GÁBOR SZEDERKÉNYI (Member, IEEE) received the M.Sc. degree in computer engineering and the Ph.D. degree in information science from the University of Pannonia, Hungary, in 1998 and 2002, respectively, and the D.Sc. degree in engineering science from the Hungarian Academy of Sciences, in 2013. He was a Researcher and a Senior Researcher at the Systems and Control Laboratory, Institute for Computer Science and Control (SZTAKI), Budapest. Since 2013, he has been a Professor in systems and control at the Faculty of Information Technology and Bionics, Pázmány Péter Catholic University, Budapest. His research interests include the analysis, identification, and control of biologically motivated nonlinear systems.